

RESSALVA

Atendendo solicitação do(a) autor(a), o texto completo desta tese será disponibilizado somente a partir de 20/03/2019.

Multifunctional platforms based on upconversion nanoparticles for applications in nanomedicine

**Thèse en cotutelle
Doctorat en chimie**

Karina Nigoghossian

Université Laval
Québec, Canada
Philosophiae doctor (Ph.D.)

et

São Paulo State University
Araraquara, Brazil
Docteur

© Karina Nigoghossian, 2018

Multifunctional platforms based on upconversion nanoparticles for applications in nanomedicine

**Thèse en cotutelle
Doctorat en chimie**

Karina Nigoghossian

Sous la direction de :

Denis Boudreau, directeur de recherche
Sidney J. L. Ribeiro, directeur de cotutelle

FICHA CATALOGRÁFICA

N684m Nigoghossian, Karina
Multifunctional platforms based on upconversion nanoparticles for applications in nanomedicine / Karina Nigoghossian. – Araraquara: [s.n.], 2018
120 p.: il.

Thesis (doctor) – Universidade Estadual Paulista, Instituto de Química
Advisor: Sidney José Lima Ribeiro
Advisor: Denis Boudreau

1. Surface plasmon resonance. 2. Biomedical materials.
3. Nanoparticles. 4. Rare earth metals. 5. Luminescence.
I. Title.

Elaboração: Seção Técnica de Aquisição e Tratamento da Informação
Biblioteca do Instituto de Química, Unesp, câmpus de Araraquara

CERTIFICADO DE APROVAÇÃO

TÍTULO DA TESE: "Plataformas multifuncionais baseadas em nanopartículas para conversão ascendente para aplicações em nanomedicina"

AUTORA: KARINA NIGOGHOSSIAN

ORIENTADOR: SIDNEY JOSE LIMA RIBEIRO


Aprovada como parte das exigências para obtenção do Título de Doutora em QUÍMICA, pela Comissão Examinadora:


Prof. Dr. SIDNEY JOSE LIMA RIBEIRO

Departamento de Química Geral e Inorgânica / Instituto de Química - UNESP - Araraquara


Prof. Dr. YOUNES MESSADDEQ

Departamento de Química Geral e Inorgânica / Instituto de Química - UNESP - Araraquara


Prof. Dr. DENIS BOUDREAU
Chemistry Department / Université Laval - Canadá



Prof. Dr. CID BARTOLOMEU DE ARAUJO

Departamento de Física / Universidade Federal de Pernambuco - Recife - PE


Prof. Dr. ANNA MARIE RITCEY
Department of Chemistry / Université Laval


Prof. Dr. MAURICIO DA SILVA BAPTISTA

Departamento de Bioquímica / Universidade de São Paulo - USP - São Paulo

unesp 

UNIVERSIDADE ESTADUAL PAULISTA

Câmpus de Araraquara



Rogéria Rocha Gonçalves

Profa. Dra. ROGÉRIA ROCHA GONÇALVES

Résumé

Dans le domaine biomédical, il y a une demande croissante pour les nanosystèmes multifonctionnels pour effectuer simultanément l'imagerie et la thérapie, en visant le diagnostic précoce et apporter du bénéfice thérapeutique maximal. Les nanoparticules à conversion ascendante d'énergie (UCNPs) ont été proposées comme une bio-sonde idéale en raison de leurs avantages uniques liés au phénomène d'*upconversion* présenté par les matériaux contenant des ions lanthanides, c'est-à-dire l'émission visible obtenue sous excitation dans le proche infrarouge (NIR), tels qu'une meilleure pénétration dans les tissus, un bas taux d'autofluorescence et un photo-dommage minimal. De plus, les propriétés luminescentes des ions lanthanides peuvent être utilisées pour la thermométrie en raison de leur forte dépendance sur la température. La thermométrie par luminescence est une technique sans contact et à haute résolution qui a attiré l'attention en nanomédecine puisque la température est un paramètre clé dans le fonctionnement des cellules. Des dommages thermiques aux cellules peuvent être localement photoinduits par l'utilisation de nanostructures métalliques illuminées dans leur bande de résonance plasmon en raison de leur absorptivité élevée. La première partie de ce travail implique le développement d'un système multifonctionnel, basé sur des nanocoquilles d'or (AuNSs) décorées avec des UCNPs, pouvant être utilisé pour augmenter et mesurer la température à l'échelle nanométrique. Ce système a été développé dans le but d'éventuelle utilisation comme agent de thérapie photothermique (PTT), dans laquelle la capacité thermométrique des UCNPs permettra d'optimiser les bénéfices thérapeutiques. La synthèse des UCNPs de NaGdF_4 dopées avec les ions Yb^{3+} et Er^{3+} a été réalisée par décomposition thermique des précurseurs de fluorure de lanthanide à des températures élevées (> 300 °C) en présence d'un ligand de coordination (l'acide oléique). Les UCNPs ont été synthétisées à trois températures différentes (310, 315 et 320 °C) et caractérisées selon leurs propriétés morphologiques, structurelles et émissives. Compte tenu des applications biologiques prévues, la surface hydrophobe des UCNPs recouverte de chaînes oléate a été modifiée par un revêtement de silice par un processus Stöber modifié au moyen d'une méthode de microémulsion inverse afin d'obtenir une dispersion suffisante dans l'eau. Des nanocristaux monodisperses de $\text{NaGdF}_4:\text{Yb}^{3+}:\text{Er}^{3+}$ à conversion ascendante (~ 25 nm de diamètre) ont été obtenus en phases cubique (à 310, 315 °C) et hexagonale (à 320 °C). Les UCNPs dans la phase hexagonale étaient plus appropriés en tant que capteurs de température en raison du rapport faible entre les émissions rouge/vert et une plus grande sensibilité thermique. Le spectre d'émission des UCNP (recouvertes de silice ou d'oléate) a été enregistré à des températures différentes à proximité de la plage physiologique (20–70 °C) et il a présenté des propriétés appropriées pour leur utilisation comme capteur de température, notamment une excellente linéarité ($R^2 > 0,99$) et une bonne sensibilité ($>3 \times 10^{-3} \text{ K}^{-1}$). La surface des AuNS a été décorée avec des UCNP recouvertes de silice. La capacité de chauffage des AuNSs@UCNPs a été vérifiée en mesurant l'émission de l' Er^{3+} , ce qui démontre leur potentiel d'application comme agent d'hyperthermie contrôlée par l'utilisation de la fonction de nanothermomètre.

La deuxième partie de ce projet de thèse a été consacrée au développement d'un nanosystème multifonctionnel pouvant être utilisé comme un système de double capture de lumière UV et de mesure de température. Le complexe $\text{Eu}(\text{tta})_3$ (tta-thénoyltrifluoroacétate) a été préparé *in situ* dans la coquille de silice des UCNPs de $\text{NaGdF}_4:\text{Yb}^{3+}:\text{Er}^{3+}$. Un nanothermomètre à double mode a été obtenu à partir du signal de fluorescence généré grâce à la conversion ascendante (proche infrarouge \rightarrow visible) par les ions Er^{3+} ainsi que par l'émission par la conversion descendante excitée dans l'UV du complexe $\text{Eu}(\text{tta})_3$. Les mesures ont été prises près de la plage de température physiologique (20–50 °C) et montrent une excellente linéarité ($R^2 > 0,99$) et une sensibilité thermique relativement élevée ($\geq 1,5\% \cdot \text{K}^{-1}$). L'utilité du complexe $\text{Eu}(\text{tta})_3$ présent dans la coquille de silice comme capteur de la lumière UV a été démontré par la dépendance de la luminescence de l'ion Eu^{3+} sur la durée de l'exposition à la lumière UV. Le matériau obtenu présente un potentiel d'application dans les thérapies activées par la lumière, telles que la thérapie photodynamique (PDT) et la PTT, qui nécessitent généralement une lumière UV ou bleue pour l'excitation. Le contrôle de la dose de lumière délivrée aux tissus a une grande importance dans ces procédures thérapeutiques pour éviter le photodommage aux tissus environnants. La fonction thermomètre est utile pour guider de tels processus (PDT et PTT) en synergie avec le dosimètre d'UV.

Mots-Clés : nanoparticules à conversion ascendante d'énergie, ions lanthanides, luminescence, nanothermométrie, hybrides organiques-inorganiques, thérapie photothermique.

Abstract

In the biomedical field, there is an increasing demand for multifunctional nanosystems to perform imaging and therapy simultaneously, aiming at early diagnosis and maximum therapeutic benefit. Upconversion nanoparticles (UCNPs) have been proposed as an ideal bio-probe because of their unique advantages related to the upconversion phenomenon presented by materials containing lanthanide ions, e.g. visible emission obtained under near-infrared (NIR) excitation, such as deep tissue penetration, low autofluorescence background and low photo-damage. Moreover, the luminescent properties of lanthanide ions may be used for thermometry because of a strongly temperature-dependent effect. Luminescence nanothermometry is a noncontact and high-resolution technique that has been gaining attention in nanomedicine since temperature is a fundamental parameter in events that occur in cells. The thermal damage of cells may be locally photoinduced by using metal nanostructures illuminated at their localized surface plasmon resonance (LSPR) band because of the enhancement of light absorption. In this work, a multifunctional system was designed combining gold nanoshells (AuNSs) and UCNPs intended as an optical heater and temperature probe at the nanoscale. This system was studied aiming its application as an agent for photothermal therapy (PTT), guided by the thermometer capacity of UCNPs, which allows to optimize the therapeutic benefits. The synthesis of NaGdF₄ UCNPs doped with ions Yb³⁺:Er³⁺ was performed via the thermal decomposition of lanthanide ion fluoride precursors at high temperatures (>300 °C) in the presence of a coordinating ligand (oleic acid). UCNPs were synthesized at three different temperatures (310, 315 and 320 °C) and characterized in terms of morphological, structural and emission properties. In view of the intended biological applications, the surface of hydrophobic oleate-capped UCNPs was modified by a silica coating to achieve sufficient water dispersibility, through a modified Stöber process by a reverse micro-emulsion method. Monodisperse NaGdF₄:Yb³⁺:Er³⁺ upconverting nanocrystals (~25 nm dia.) were obtained in cubic (at 310, 315 °C) and hexagonal phase (at 320 °C). The UCNPs in the hexagonal phase showed to be more suitable for application as a temperature sensor, because of its lower red-to-green emission ratio and higher thermal sensitivity. The emission spectra of NaGdF₄:Yb³⁺:Er³⁺ (oleate- or silica-coated) UCNPs were measured at different temperatures in the vicinity of the physiological temperature range (20-70 °C) and presented suitable properties for application as a temperature sensor, such as excellent linearity ($R^2 > 0.99$) and sensitivity ($> 3 \times 10^{-3} \text{ K}^{-1}$). The surface of AuNSs were decorated with silica-coated UCNPs. The heating capacity of such nanocomposites (AuNSs@UCNPs) was verified by monitoring the Er³⁺ emission, enabling potential application as a hyperthermia agent controlled by the nanothermometer function. In a second part of this thesis, a multifunctional nanosystem was designed and applied as a dual sensor of ultraviolet (UV) light and temperature. Eu(tta)₃ (tta-thenoyltrifluoroacetate) complex was prepared *in situ* over the silica shell of NaGdF₄:Yb³⁺:Er³⁺ UCNPs. A dual-mode nanothermometer-UV sensor was obtained from the combination of NIR to visible upconversion fluorescence signal of Er³⁺ ions and the UV-excited downshifted emission

from the $\text{Eu}(\text{tta})_3$ complex. Measurements were performed near the physiological temperature range (20-50 °C) revealing excellent linearity ($R^2 > 0.99$) and relatively high thermal sensitivities ($>1.5\% \cdot \text{K}^{-1}$). The $\text{Eu}(\text{tta})_3$ complex present in the silica shell was also demonstrated as a UV sensor because of the Eu^{3+} luminescence dependence on UV light exposure. The obtained material shows potential for application in light activated therapies, such as photodynamic therapy (PDT) and PTT, which typically require UV or blue light for excitation. The control of light dose released to the tissue is of great importance in these therapeutic procedures to avoid photodamage to the surroundings. The thermometer function is useful to guide such therapeutic processes (PDT and PTT) synergistically with the UV dosimeter.

Keywords: upconversion nanoparticles, lanthanide ions, luminescence, nanothermometry, organic-inorganic hybrids, photothermal therapy.

Resumo

Na área biomédica, existe uma crescente demanda por nanossistemas multifuncionais para realização de imageamento e terapia simultaneamente, visando um diagnóstico precoce e máximo benefício terapêutico. Nanopartículas para conversão ascendente de energia (UCNPs) vêm sendo propostas como a sonda biológica ideal devido às suas vantagens únicas relacionadas ao fenômeno de *upconversion* apresentado por materiais contendo íons lantanídeos, isto é, emissão no visível obtida sob excitação no infravermelho, tais como penetração profunda nos tecidos, uma baixa taxa de autofluorescência e um fotodano mínimo. Além disso, as propriedades luminescentes dos íons lantanídeos podem ser usadas para termometria por serem fortemente dependentes da temperatura. A termometria luminescente é uma técnica de não-contato e alta resolução que vem ganhando atenção na nanomedicina uma vez que a temperatura é um parâmetro fundamental para o funcionamento das células. Danos térmicos às células podem ser localmente fotoinduzidos pelo uso de nanoestruturas metálicas iluminadas em sua banda de ressonância plasmônica por causa da sua elevada absorvidade. A primeira parte deste trabalho consiste no desenvolvimento de um sistema multifuncional baseado em nanocascas de ouro (AuNSs) decoradas com UCNPs podendo ser utilizadas para aumentar e medir a temperatura em escala nanométrica. Este sistema foi desenvolvido com a finalidade de uma eventual utilização como agente em terapia fototérmica (PTT), na qual a capacidade termométrica das UCNPs permitirá otimizar os benefícios terapêuticos. A síntese das UCNPs de NaGdF_4 dopadas com os íons Yb^{3+} e Er^{3+} foi realizada via decomposição térmica de precursores de fluoreto de lantanídeo a altas temperaturas ($> 300\text{ }^\circ\text{C}$) na presença de um ligante coordenante (o ácido oleico). As UCNPs foram sintetizadas em três diferentes temperaturas (310, 315 e $320\text{ }^\circ\text{C}$) e caracterizadas segundo suas propriedades morfológicas, estruturais e emissivas. Levando-se em conta as aplicações biológicas pretendidas, a superfície hidrofóbica das UCNPs recoberta por cadeias de oleato foi modificada utilizando um revestimento de sílica via um processo Stöber modificado por meio de um método de microemulsão reversa para obter uma dispersão suficiente em água. Nanocristais monodispersos de $\text{NaGdF}_4:\text{Yb}^{3+}:\text{Er}^{3+}$ para conversão ascendente ($\sim 25\text{ nm}$ de diâmetro) foram obtidos nas fases cúbica (a $310, 315\text{ }^\circ\text{C}$) e hexagonal (a $320\text{ }^\circ\text{C}$). As UCNPs na fase hexagonal mostraram-se mais apropriadas como sensores de temperatura, devido a menor razão entre as emissões vermelho/verde e maior sensibilidade térmica. O espectro de emissão das UCNPs (recobertas por sílica ou por oleato) foi registrado a diferentes temperaturas na proximidade do intervalo fisiológico ($20\text{--}70\text{ }^\circ\text{C}$) e apresentou propriedades adequadas para sua aplicação como sensor de temperatura, especialmente uma excelente linearidade ($R^2 > 0,99$) e uma boa sensibilidade ($>3 \times 10^{-3}\text{ K}^{-1}$). A superfície das AuNSs foi decorada com UCNPs recobertas por sílica. A capacidade de aquecimento das AuNSs@UCNPs foi verificada medindo-se a emissão do Er^{3+} , a qual demonstra seu potencial como agente em hipertermia controlada pela utilização da função de nanotermômetro. A segunda parte deste projeto de tese foi dedicada ao desenvolvimento de um nanossistema multifuncional podendo ser utilizado como um sistema

de dupla captura de luz UV e medida de temperatura. O complexo $\text{Eu}(\text{tta})_3$ (tta-tenoiltrifluoroacetato) foi preparado *in situ* na casca de sílica das UCNPs de $\text{NaGdF}_4:\text{Yb}^{3+}:\text{Er}^{3+}$. Um nanotermômetro de modo duplo foi obtido a partir do sinal de fluorescência gerado graças à conversão ascendente (infravermelho próximo \rightarrow visível) pelos íons Er^{3+} juntamente à emissão por conversão descendente excitada no UV do complexo $\text{Eu}(\text{tta})_3$. As medidas foram realizadas próximo à faixa de temperatura fisiológica (20—50 °C) revelando uma excelente linearidade ($R^2 > 0,99$) e uma sensibilidade térmica relativamente alta ($\geq 1,5\% \cdot \text{K}^{-1}$). A utilidade do complexo de $\text{Eu}(\text{tta})_3$ presente na casca de sílica como sensor de luz UV foi demonstrado pela dependência da luminescência do íon Eu^{3+} sob a duração da exposição à luz UV. O material obtido apresenta potencial para aplicação em terapias ativadas pela luz, tais como a terapia fotodinâmica (PDT) e a PTT, as quais tipicamente requerem luz UV ou azul para excitação. O controle da dose de luz liberada para os tecidos tem grande importância nestes procedimentos terapêuticos para evitar o fotodano aos tecidos circundantes. A função de termômetro é útil para guiar tais processos (PDT e PTT) simultaneamente com o dosímetro de UV.

Palavras-chave: nanopartículas para conversão ascendente de energia, íons lantanídeos, luminescência, nanotermometria, híbridos orgânicos-inorgânicos, terapia fototérmica.

Contents

Résumé	v
Abstract	vii
Resumo	ix
List of figures	xiv
List of tables	xvi
List of abbreviations and symbols	xvii
Acknowledgments	xx
Foreword	xxiii
Chapter 1. General introduction and statement of the problem	27
1.1. Multifunctional theranostic nanosystems	27
1.2. Luminophores for biomedical applications	28
1.3. Lanthanide-based upconversion nanoparticles	29
1.4. Lanthanide-based luminescent nanothermometry	30
1.5. Photothermal therapy	32
1.6. Multifunctional systems for luminescent thermometry and plasmonic heating	32
References	33
Chapter 2. Theory and review of literature	41
2.1. Basic mechanisms of photoluminescence	41
2.2. Lanthanide photoluminescence properties	42
2.3. Upconversion luminescence mechanisms	43
2.4. Temperature measurement	45
2.5. Luminescence thermometry	46
2.6. Gold nanoparticles for bioapplications	48
References	50
Chapter 3. Objectives	56
3.1. General objective	56
3.2. Specific objectives	56
Chapter 4. Methods	58
4.1. Synthesis procedures	58
4.1.1. Thermal decomposition synthesis	58
4.1.1.1. Synthesis of Gd ³⁺ :Yb ³⁺ :Er ³⁺ trifluoroacetate precursor	58
4.1.1.2. Synthesis of Yb ³⁺ :Er ³⁺ co-doped NaGdF ₄ UCNPs	58
4.1.2. Silica coating of NaGdF ₄ :Yb ³⁺ :Er ³⁺ UCNPs	59
4.1.3. Synthesis of UCNP-metal nanocomposites	59
4.1.4. In situ preparation of the complex Eu(tta) ₃ at the silica shell of UCNPs	60
4.2. Characterizations	60
4.2.1. Structural characterization	60
4.2.2. Optical characterization	61
4.2.3. Temperature sensing	61
4.2.3.1. Er ³⁺ emission-based thermometer	61
4.2.3.2. Eu ³⁺ emission-based thermometer	62
4.2.3.3 Thermal sensitivity	63
4.2.4. Photothermal effect	64
4.2.5. UV light sensing	64
References	64

Chapter 5. Upconversion nanoparticle-decorated gold nanoshells for near-infrared induced heating and thermometry.....	67
Résumé	67
Resumo	67
Abstract	68
5.1. Introduction.....	68
5.2. Experimental details.....	70
5.2.1 Materials.....	70
5.2.2. Synthesis of Yb ³⁺ :Er ³⁺ co-doped NaGdF ₄ UCNPs.....	70
5.2.3. Silica coating of NaGdF ₄ :Yb ³⁺ :Er ³⁺ UCNPs.....	71
5.2.4. Synthesis of SiO ₂ @Au nanoshells	71
5.2.4.1. Silica cores.....	71
5.2.4.2. SiO ₂ @NH ₂	71
5.2.4.3. Gold seeds	71
5.2.4.4. SiO ₂ @seeds.....	72
5.2.4.5 Shell growth	72
5.2.5. Synthesis of nanocomposite AuNSs@UCNPs	72
5.2.5.1. UCNPs@SiO ₂ -NH ₂	72
5.2.5.2. UCNP attachment on AuNSs	72
5.2.6. Morphological and structural characterization	73
5.2.7. Optical characterization.....	73
5.2.8. Temperature sensing.....	73
5.2.9. Photothermal effect	73
5.3. Results and discussion	73
5.3.1. Oleate-capped NaGdF ₄ :Yb ³⁺ :Er ³⁺ UCNPs	73
5.3.2. Silica-coated NaGdF ₄ :Yb ³⁺ :Er ³⁺ UCNPs.....	76
5.3.3. Temperature sensing.....	77
5.3.4. Photothermal effect	80
5.4. Conclusions	83
References	83
Chapter 6. UV and temperature-sensing based on NaGdF₄:Yb³⁺:Er³⁺@SiO₂-Eu(tta)₃	87
Résumé	87
Resumo	87
Abstract	88
6.1. Introduction.....	88
6.2. Materials and methods.....	89
6.2.1. Materials.....	89
6.2.2. Synthesis of Yb ³⁺ :Er ³⁺ co-doped NaGdF ₄ UCNPs.....	89
6.2.3. Silica coating of NaGdF ₄ :Yb ³⁺ :Er ³⁺ UCNPs.....	90
6.2.4. Preparation of NaGdF ₄ :Yb ³⁺ :Er ³⁺ @SiO ₂ -Eu(tta) ₃	90
6.2.5. Characterization	91
6.3. Results and discussion	91
6.4. Conclusions	98
References	99
Chapter 7. Upconversion nanocomposites for PDT	104
7.1. Introduction.....	104
7.2. Materials and methods.....	107
7.2.1 Materials.....	107

7.2.2. Preparation of UCNPs@SiO ₂ -PS	107
7.2.3. PDT assays	107
7.3. Results and discussion	108
7.4. Conclusions	114
References	115
Chapter 8. Conclusions	118
References	120

List of figures

Figure 2.1. Energy level scheme for a simplified representation of luminescence process.....	42
Figure 2.2. Mechanisms to convert low-energy photon pump sources into higher energy output: Simultaneous two-photon absorption (STPA), Second-harmonic generation (SHG), Upconversion (UC). The horizontal dashed (solid) lines indicate virtual (discrete) levels.....	44
Figure 2.3. Energy transfer mechanisms: excited state absorption (ESA) and energy transfer upconversion (ETU). (S: sensitizer ion, A: activator ion)	44
Figure 2.4. Extinction spectra of aqueous solutions of gold nanoparticles in different shapes: spheres, rods and shells.....	49
Figure 4.1. Schematic energy-level diagram of Yb ³⁺ and Er ³⁺ and mechanism of upconversion emissions under 980 nm laser excitation.....	62
Figure 4.2. Schematic energy-level diagram showing the mechanism of energy transfer from tta to Eu ³⁺ and downshifting emission under UV excitation.....	63
Figure 5.1. (a) TEM images of NaGdF ₄ :Yb ³⁺ :Er ³⁺ nanoparticles prepared at 310, 315 and 320 °C and (b) their respective particle size distributions.	74
Figure 5.2. XRD patterns of NaGdF ₄ :Yb ³⁺ :Er ³⁺ UCNPs prepared at different temperatures. Reference diffraction peaks corresponding to cubic and hexagonal NaGdF ₄	75
Figure 5.3. Upconversion emission spectra obtained using 980 nm laser pumping at different powers for α-UCNPs (a) and β-UCNPs (c). Integrated intensity (areas) vs. pumping intensity for α-UCNPs (b) and β-UCNPs (d).	76
Figure 5.4. (a) TEM image and (b) particle-size distribution of silica-coated UCNPs.	77
Figure 5.5. Schematic energy level diagram of Yb ³⁺ and Er ³⁺ and the mechanism of upconversion emissions under 980 nm laser excitation.	78
Figure 5.6. Upconversion emission spectra (λ _{exc.} 980 nm) at different temperatures (20–70 °C) of α-UCNPs (a), β-UCNPs (b), and β-UCNPs@SiO ₂ (c). Boltzmann's plots (d).	79
Figure 5.7. Thermal sensitivities of α-UCNPs, β-UCNPs and silica-coated β-UCNPs.	80
Figure 5.8. (a) TEM image and (b) extinction spectrum of AuNSs@UCNPs.	81
Figure 5.9. Upconversion emission spectra (λ _{exc.} 980 nm) for different laser powers of AuNSs@UCNPs (a) and UCNPs@SiO ₂ (b). Calculated temperature values (c).	82
Figure 6.1. TEM images of (a) UCNPs and (b) UCNPs@SiO ₂ . (c) X-ray diffraction pattern and reference diffraction peaks corresponding to hexagonal NaGdF ₄ (JCPDS file 27-0699). (d) Upconversion emission spectra (λ _{exc.} 980 nm) at different temperatures (293 and 323 K) of UCNPs@SiO ₂	92

Figure 6.2. (a) Excitation (λ_{em} 615 nm) and (b) emission spectra for the complex [Eu(tta) ₃ (H ₂ O) ₂] (black), the compound [Eu(tta) ₃ -host] (red), and UCNPs@SiO ₂ -Eu(tta) ₃ (blue). Spectra of [Eu(tta) ₃ (H ₂ O) ₂] and [Eu(tta) ₃ -host] were adapted from Molina <i>et al.</i>	93
Figure 6.3. Emission spectra of UCNPs@SiO ₂ -Eu(tta) ₃ at different temperatures (293–323 K): under (a) UV and (b) NIR excitation. Insets: Corresponding luminescent photographs. Thermal calibration curves: (c) fluorescence intensity (integrated area) vs temperature (λ_{exc} 352 nm) and (d) ln(FIR) vs inverse temperature (λ_{exc} 980 nm).	94
Figure 6.4. Linear function between real and calculated temperature for Er ³⁺ - and Eu ³⁺ -based thermometers.	95
Figure 6.5. Relative thermal sensitivity (S_r) as a function of temperature for Er ³⁺ /Yb ³⁺ system (green) and for Eu(tta) system (red).	96
Figure 6.6. Upconversion emission spectra (λ_{exc} . 980 nm) and calculated temperature values at different laser powers.	97
Figure 6.7. (a) Emission spectra (λ_{exc} 352 nm) of UCNPs@SiO ₂ -Eu(tta) ₃ after different periods of exposure to UV light. (b) Fluorescence intensity (integrated area) under UV (352 nm) and NIR (980 nm) excitation and fluorescence intensity ratio between Eu ³⁺ and Er ³⁺ emissions vs time (the solid line represents the exponential fit curve).	98
Figure 7.1. Jablonski diagram adapted for a typical photoactivation process. Vibrational sub-levels are not shown for reasons of clarity.	105
Figure 7.2. Chemical structures of halogen-xanthene PDT sensitizers used in the present work.	106
Figure 7.3. TEM image and particle-size distribution of UCNPs@SiO ₂ -PS.	108
Figure 7.4. Absorption spectra of ethanolic solution of PSs (eosin, erythrosin and rose bengal) and upconversion emission spectrum of UCNPs (NaGdF ₄ :Yb ³⁺ :Er ³⁺ @SiO ₂).....	109
Figure 7.5. Absorption spectra for initial PS solution (black) and for the supernatant collected after the incorporation for UCNPs@SiO ₂ (red) and UCNPs@SiO ₂ -NH ₂ (blue) for three initial PS concentrations (10, 50 and 100 nM).	110
Figure 7.6. Excitation (green) and emission (red) spectra for PS-containing UCNPs@SiO ₂	111
Figure 7.7. Upconversion emission spectra pumping at different powers for PS-containing UCNPs@SiO ₂ with concentrations: 10, 50 and 100 nM.	112
Figure 7.8. Red-to-green emission intensity ratio for UCNPs@SiO ₂ -PS (10, 50 and 100 are PS concentrations in nM). Control: PS-free UCNPs@SiO ₂	113
Figure 7.9. Singlet oxygen decay curve and exponential fit for EO (λ_{exc} 516 nm), ER (λ_{exc} 526 nm) and RB (λ_{exc} 549 nm) in UCNPs@SiO ₂ dispersions in D ₂ O with PS concentrations of 10, 50 and 100 nM. Control: PS free in D ₂ O solution.	114

List of tables

Table 6.1. Calibration parameters of the dual-mode thermometer under UV and NIR excitations.	96
Table 6.2. Maximum relative thermal sensitivity of Yb ³⁺ :Er ³⁺ doped UCNPs.	97
Table 6.3. Maximum relative thermal sensitivity of Eu ³⁺ -based thermometers.	97
Table 7.1. Maximum excitation and emission wavelengths for PS-containing UCNPs@SiO ₂	111
Table 7.2. Singlet oxygen lifetimes (τ) obtained from decay curves for the samples.	114

List of abbreviations and symbols

$^1\text{O}_2$	singlet oxygen
α	crystal cubic phase
β	crystal hexagonal phase
λ	wavelength
λ_{em}	emission wavelength
λ_{exc}	excitation wavelength
ν	frequency
∂T	temperature uncertainty
A	active luminescent center in the ground state
A*	active luminescent center in the excited state
Abs _{free}	absorbance of PS free in solvent
Abs _{initial}	absorbance of PS initial solution
A _{ji}	spontaneous emission rate
APTES	(3-aminopropyl)triethoxysilane
AuNSs	gold nanoshells
BC	bacterial cellulose
CIAIPc	chloroaluminum phtalocyanine
D ₂ O	deuterium oxide
DLS	dynamic light scattering
E	energy of the level
ΔE	energy gap separating two excited states
EO	eosin B
EPR	enhanced permeation and retention
ER	erythrosine B
ESA	excited-state absorption
ETU	energy transfer upconversion
FIR	fluorescence intensity ratio
g	degeneracy of the state
GFP	green fluorescent protein

h	Planck constant
HE	haematoxylin and eosin
ICDD	International Centre for Diffraction Data
I_{em}	intensity of emission
I_{ex}	pumping intensity
ISC	intersystem crossing
JCPDS	joint committee on powder diffraction standards
k_B	Boltzmann constant
Ln^{3+}	trivalent lanthanide ions
MSNPs	mesoporous silica nanoparticles
n	number of infrared photons
NIR	near-infrared
NIR-I	first biological window
NIR-II	second biological window
NIR-III	third biological window
NR	non-radiative pathway
OIH	organic-inorganic hybrid
OPO	optical parametric oscillator
PEG	polyethylene glycol
PDT	photodynamic therapy
PL	photoluminescence emission spectrum
PLE	photoluminescence excitation spectrum
PS	photosensitizer
PTT	photothermal therapy
Q	experimental parameter
QDs	quantum dots
R	radiative pathway
R^2	regression coefficient
RB	rose bengal
RSD	relative standard deviation
S	absolute thermal sensitivity

S₀	singlet ground state
S₁	singlet excited state
S_r	relative thermal sensitivity
SERS	surface-enhanced Raman scattering
SHG	second-harmonic generation
SPR	surface plasmon resonance
STPA	simultaneous two-photon absorption
T	absolute temperature
TEM	transmission electron microscopy
TEOS	tetraethylorthosilicate
T₁	triplet excited state
tta	thenoyltrifluoroacetate
UC	upconversion
UCNPs	upconversion nanoparticles
UCNPs@SiO₂	silica coated upconversion nanoparticles
UV	ultraviolet
XRD	X-ray diffraction

Acknowledgments

I am deeply grateful to my supervisor Prof. Dr. Sidney José Lima Ribeiro, who guided me since I was an undergraduate student, having a huge role in my professional development. Although today I cannot see myself doing anything but academic research, since the beginning he gave me the freedom to fulfill or not this fated destiny in science by encouraging me to experience different work fields – from industry to volunteering –, and by allowing me to collaborate with diverse research groups in Brazil and abroad. My way back to research always occurred spontaneously, and thus make me feel safe about my present career choices. I am also grateful to him for giving me autonomy to conceive this thesis, for always propose new ideas, discuss the results and patiently review the manuscripts. And for never doubting my ability to handle very broad research topics, despite my pharmaceutical background.

I would like to express my sincere gratitude to my supervisor Prof. Dr. Denis Boudreau for the continuous support and guidance. For his trust in my work by giving me opportunity to be part of his group. For being always concerned about the management and progress of the research, the students' motivation and the integration of group members, while always keeping a pleasant environment. For carefully reading earlier drafts of this thesis and other scientific texts and giving valuable feedback. And specially for teaching me that I am in control of my work, not the opposite.

I also want to thank Prof. Dr. Younès Messaddeq for the continuous support of my PhD studies, for the essential efforts to make this cotutelle possible and for the warm reception in Québec along with Dr. Sandra Helena Messaddeq. I am glad to still be professionally involved with my very first professor of General and Inorganic Chemistry in the early days of Pharmacy School, one of the most inspiring personalities I have met, being an example of motivation, enthusiasm, and immense knowledge. I cannot fail to mention about how grateful I am to him for giving me the once in a lifetime opportunity to go to France in 2008 in a journey of self-discovery, in one of the most inspirational research experiences I had.

Besides my supervisors, I would like to thank the rest of my thesis committee: Prof. Dr. Cid B. de Araújo, Prof. Dr. Rogéria R. Gonçalves, Prof. Dr. Mauricio S. Baptista and Prof. Dr. Anna Ritcey, for reviewing the written work, for participating in the final oral examination, and for the valuable comments, criticisms and suggestions that brought insights from different perspectives. Specially, Prof. Dr. Mauricio S. Baptista, who gave access to the laboratory and research facilities. I am grateful for the stimulating discussions and for opening a new perspective for my work during the last year of my PhD.

I thank Prof. Dr. Claudine Allen for permitting me to use lab facilities for the synthesis of nanoparticles and the group members Dr. Marie-Ève Lecavalier, Dr. Sébastien Lamarre and Dr. Marc-Antoine Langevin for helping me in the lab.

I thank my kind fellow labmates from Boudreau's group: Dr. Samuel Ouellet, Dr. Jérémie Asselin, Dr. Alexandre Grégoire, Dr. Josée Richard-Daniel, Dr. Félix-Antoine Lavoie, Philippe Legros, Marie-Pier Lambert, Mélina Drouin, Alexe Grenier, Nicolas Fontaine, Lydia Parent, Marie-Pier Côté. I learned so

much from you, whether in the exciting group meetings or during the fun moments in the lab, that I was always worried about how I could contribute back to my colleagues. I learnt that in a group in which everyone recognizes the qualities of each other, there is no place for competition and the synergism bring excellent results for the team.

I also thank my colleagues from Messaddeq's group: Dr. Yannick Ledemi, Dr. Mathilde Loubier, Dr. Maxime Rioux, Dr. Hssen, Dr. Guilherme Marcondes, Dr. Otávio De Brito Silva and Dr. Rim Baklouti.

I thank colleagues that became friends for life from the Laboratory of Photonic Materials (Unesp): Prof. Dr. Danilo Manzani, Dr. Gustavo Galleani, Dr. Sílvia H. Santagneli, Dr. Chanchal Hazra, Dr. Sybele Saska, Dr. Hssen Fares, Dr. Hernane Barud, Dr. Rafael Miguel Sábio, Dr. Molíria V. dos Santos, Dr. Robson Rosa da Silva, Dr. Denise de Salvi, Dr. Maurício Cavicchioli, Livia M. Christovam, Laís Galvão, Laís Roncalho, Fernando Maturi, Juliane Resges Orives, Andreia Monteiro, Samira Stain, York Correales, César Polachini, Tâmara J. Oliveira, Prof. Dr. Sajjad Khan, Prof. Dr. Camila Pereira, Prof. Dr. Mauricio Caiut, Prof. Dr. Édison Pecoraro and Prof. Dr. Marcelo Nalin, among so many others that I crossed paths with in this lab in more than a decade.

To the staff of the Institute of Chemistry of Unesp for the commitment to professional formation of the students and continuous improvement, specially to Dr. Sérgio Luís Scarpari, Rafael R. Domeneguetti, Luiz F. Aquino, Valéria C. M. Bizelli and Wennia L. S. dos Santos.

Juninho Moura Basque for the friendship, for helping me to improve my communication skills in so many languages and for constant psychological support.

I would to express my appreciation to my family: my parents Lilian and Rubens, to my brother Rubinho and my sister in law Violeta for inspiring me and for moral support throughout my life in general. I also thank my dear friends Dayana, Josiane, Priscila and Sílvia for being by my side and for bringing happiness to my life.

Finally, I acknowledge the financial support from Brazilians Agencies FAPESP and CAPES-CNPq (process numbers 99999.010867/2014-07 and 141253/2014-2). The Natural Sciences and Engineering Research Council of Canada and the *Fonds de recherche du Québec-Nature et Technologies* are also acknowledged for their financial support.

To all the women who walk down their own paths in considerable disadvantage
and fight daily for their independence.
May we evolve towards equality strengthened by our differences.
Together we will be stronger.

Foreword

This thesis has been developed under a cotutelle program between Université Laval (Québec, Canada) and São Paulo State University (Araraquara, Brazil) under the supervision of Prof. Denis Boudreau and Prof. Sidney J. L. Ribeiro in the scope of the Joint International Research Unit (JIRU) UNESP-Laval. The purpose of the project was to investigate the use of lanthanide-based luminescent nanoparticles for UV-sensing and nanothermometry combined with gold nanoshell-based photothermal therapy in multifunctional nanosystems aiming for biomedical applications.

This thesis is structured in chapters as follows:

Chapter 1 brings a general introduction on how nanotechnology allows the development of multifunctional nanoparticles and to contextualize the quite recent theranostic nanomedicine concept, an integration of diagnostics and therapy in a single nanoplatform seeking to maximize the therapeutic benefits. The components of such system are presented, more specifically the conventional luminescent probes and the advantages of lanthanide-based upconversion nanoparticles for biomedical applications. In addition to the bioimaging function, the use of lanthanides luminescence for nanothermometry and the UCNP-metal nanocomposites as multifunctional system for nanomedicine are addressed.

Chapter 2 is focused on theory and review of literature, which start from the basic mechanisms of photoluminescence and then provide the principles of lanthanide photoluminescence with an emphasis on the theory for upconversion luminescence of lanthanide ions. The aspects of temperature measurement techniques are discussed. Special attention is given to the various methods of luminescence thermometry with a focus on biological applications. A comprehensive overview of the use of gold nanoparticles for biomedical application in photothermal therapy is given.

The main motivations and goals of this thesis are highlighted in Chapter 3, as well as the specific objectives that must be met in order to achieve the intended research contribution. Chapter 4 provides the fundamentals behind the experimental methodology chosen concerning the synthesis of nanomaterials and the post-synthesis surface modification strategies, and the characterization methodology used to investigate structural and optical properties as well as the promising applications in thermometry and UV light sensing. The results and discussions obtained generated two scientific papers, presented in Chapters 5 and 6. Chapter 7 presents additional results concerning the development of a upconversion-based nanosystem for use in photodynamic therapy. Chapter 8 concludes the thesis.

Chapter 5 presents the article “Upconversion nanoparticle-decorated gold nanoshells for near-infrared induced heating and thermometry”. This work was devoted to the use of lanthanides and metallic particles for applications in nanomedicine as heater and thermometer under near-infrared excitation. This new nanopatform is dispersible in an aqueous environment, thus being attractive for guiding light activated hyperthermia therapies to avoid overheating of normal tissues. Modifications with respect to the original article consists of additional paragraph in Section 5.3 about the temperature reaction effect on nanoparticles morphology, size and phase.

Publication details

Authors: Karina Nigoghossian, Samuel Ouellet, Jérôme Plain, Younès Messaddeq, Denis Boudreau, Sidney José Lima Ribeiro

Journal: Journal of Materials Chemistry B

Submitted: 13th June 2017

Accepted: 1st August 2017

Published: 2nd August 2017

DOI: 10.1039/c7tb01621b

The work “UV and temperature-sensing based on $\text{NaGdF}_4:\text{Yb}^{3+}:\text{Er}^{3+}@\text{SiO}_2\text{-Eu}(\text{tta})_3$ ” is addressed in Chapter 6. In this paper, the use of lanthanides for sensing applications was explored. The obtained material presented multiple applications in luminescent thermometry, under ultraviolet or near-infrared excitation, and in UV light sensing for applications in nanomedicine to avoid photodamage and excessive heating of non-targeted tissues. Additional information, not present in the original article, are: (i) Linear function between real and calculated temperature for Er^{3+} - and Eu^{3+} -based thermometers (Figure 6.4); (ii) Relative thermal sensitivity (S_r) as a function of temperature for $\text{Er}^{3+}/\text{Yb}^{3+}$ system (green) and for $\text{Eu}(\text{tta})$ system (red) (Figure 6.5); (iii) Maximum relative thermal sensitivity of $\text{Yb}^{3+}:\text{Er}^{3+}$ doped UCNPs (Table 6.2); (iv) Maximum relative thermal sensitivity of Eu^{3+} -based thermometers (Table 6.3); and (v) Upconversion emission spectra ($\lambda_{\text{exc.}}$ 980 nm) and calculated temperature values at different laser powers (Figure 6.6).

Publication details

Authors: Karina Nigoghossian, Younès Messaddeq, Denis Boudreau, Sidney José Lima Ribeiro

Journal: ACS Omega

Submitted: 16th January 2017

Accepted: 3rd May 2017

Published: 15th May 2017

DOI: 10.1021/acsomega.7b00056

The author of this thesis wrote the research project for the evaluation of postgraduate programs of both universities, conceived the experimental plan, performed the experimental work of synthesis and characterization of obtained samples, analyzed the results, presented preliminary findings at the groups meetings, wrote draft manuscripts, and is thus the first author of both manuscripts. The experimental part was performed at the laboratories of the following professors: Prof. Sidney J. L. Ribeiro, head of the Laboratory of Photonic Materials, in the Institute of Chemistry (UNESP) with expertise in luminescent lanthanide-based materials; Prof. Denis Boudreau at Université Laval, who has been heading the investigation of surface plasmon resonance effects in nanoparticle systems for several years; and Prof. Younès Messaddeq, who leads the research activities on materials for optics and photonics including nanostructured materials at the Centre of Optic Photonic and Lasers (COPL), Université de Laval, Québec, Canada. These professors provided guidance for all activities mentioned above, proposing ideas, discussing the results and reviewing the manuscripts, reports and thesis redaction. Samuel Ouellet prepared gold nanoshells samples following a methodology that he developed during his PhD at Prof. Jérôme Plain's laboratory at Université de Technologie de Troyes in France.

The main results were presented in the following conferences:

1. Nigoghossian, K.; Vorpapel, A. J.; Peres, M. F. S.; Primo, F. L.; Tedesco, A. C.; Pecoraro, E.; Messaddeq, Y.; Ribeiro, S. J. L. "Bacterial cellulose-yttrium vanadate nanoparticles composite membranes", at XIII Brazilian Materials Research Society Meeting, João Pessoa, PB, Brazil, 2014 (Oral presentation).
2. Nigoghossian, K.; Ribeiro, S. J. L.; Messaddeq, Y.; Boudreau, D. "Nanoscale thermometry based on core-shell upconverting nanoparticles for biological applications", at 7th International Conference on Optical, Optoelectronic and Photonic Materials and Applications (ICOOPMA 2016), Montréal, QC, Canada, 2016 (Poster presentation).
3. Nigoghossian, K.; Ouellet, S.; Ribeiro, S. J. L.; Messaddeq, Y.; Boudreau, D. "Luminescent nanothermometers based on upconversion nanoparticles for applications in nanomedicine." at XVIII BMIC Brazilian Meeting on Inorganic Chemistry and 7th Brazilian Meeting on Rare Earths, São Pedro, SP, Brazil, 2016 (Oral presentation).
4. Nigoghossian, K.; S.; Messaddeq, Y.; Boudreau, D.; Ribeiro, S. J. L. "Dual-sensor of UV-light and temperature based on $\text{NaGdF}_4:\text{Yb}^{3+}:\text{Er}^{3+}@\text{SiO}_2\text{-Eu}(\text{tta})_3$ nanoparticles" at 10th International Conference on Nanophotonics (ICNP), Recife, PE, Brazil, 2017 (Poster presentation).
5. Nigoghossian, K.; S.; Messaddeq, Y.; Boudreau, D.; Ribeiro, S. J. L. "UV and temperature sensing based on $\text{NaGdF}_4:\text{Yb}^{3+}:\text{Er}^{3+}@\text{SiO}_2\text{-Eu}(\text{tta})_3$ nanoparticles" at Spectral shaping for biomedical and energy applications (SHIFT), Tenerife, Canary Islands, Spain, 2017 (Poster presentation).

"All sudden understanding is finally the revelation of an acute incomprehension."
Clarice Lispector

Chapter 1.

General introduction and statement of the problem

1.1. Multifunctional theranostic nanosystems

Current research in the biomedical field is focused on the needs for early and accurate diagnosis, as well as minimally invasive, more efficient, less toxic and fast response treatment techniques. In this direction, nanomedicine is a growing field in which the nanotechnology is applied to pharmaceutical and biomedical sciences to improve the efficacy and safety of conventional medicine.^{1,2} Nanometer-scale materials can interact with biological entities in the same (1–100 nm) or close scale length in processes that involve molecules, cells and tissues. Therefore, the use of nanomaterials is a tool to obtain target selectivity and spatiotemporal controlled therapy or sensing.^{3–5}

The recent advances in nanotechnology has enabled the fabrication of engineered nanoparticles with tunable optical, electrical and magnetic features by controlling their size, shape, surface chemistry and physicochemical properties.⁶ In the biological environment, these features determines the particles' interactions with biological components, such as adsorption of ions and proteins, cellular uptake, biodistribution, and clearance mechanisms.⁷ For instance, particle size is a critical parameter that dictates whether the clearance occurs rapidly through the kidneys followed by urinary excretion (<10 nm) or whether a more complex clearance mechanism occurs *via* the liver (>10 nm).^{8,9} Administration of therapeutic agents in nanoparticles not only prevents its loss of function by degradation or denaturation, but also modulates the pharmacodynamics and pharmacokinetics, minimizing undesirable side effects.¹⁰

Specific properties may be combined in a single composite material to obtain a multifunctional platform, in which each component performs its respective function, or they can act synergistically to produce an enhanced effect.^{11–14} The development of multifunctional nanosystems for integrated diagnosis and treatment is a growing research field in nanomedicine recently named as theranostic.¹⁵ The multitask particles are aimed to perform diagnosis, drug delivery or therapy activation, and monitoring the therapeutic responses in real time, thus maximizing the therapeutic benefits. The assembly of components in well-defined nanostructures must preserve each function. The core-shell structure is the adequate one for biological applications since the particle dispersion is essential. Such systems usually combine an imaging component at the core, surrounded by a carrier shell able to encapsulate therapeutic agents, and

with a chemically reactive surface to allow for functionalization with a targeting agent for cellular recognition.¹⁶

The design of carriers for drug delivery explores primarily liposomes¹⁷ and polymers¹⁸. Rigid nanoparticles may be used as well.¹⁹ Within them, those based on SiO₂ are by far the most widely used and detailed *in vivo* toxicity studies have been performed.^{20–24} Mesoporous silica nanoparticles (MSNPs) with tuned pore-size distribution, pore geometry, and pore network tortuosity, ordered arrays, as well as radial dendritic structures can be achieved by controlling the synthesis parameters.²⁵ Specific molecules can be retained in pores by electrostatic interactions or H-bonds, as well as by reversible chemical reactions.^{26–28} Once in the cytoplasm, the encapsulated molecules can be passively released by mere desorption, by erosion of MPSN or by a combination of both.²⁹ This process can be triggered by changes in pH,^{30–32} temperature,^{33,34} light irradiation,^{35,36} magnetic field³⁷ or complementary molecules or functional groups.^{38–40}

Concerning targeting strategies, the leaky tumor blood vasculature makes the nanoparticles preferentially accumulate into tumor tissues than their normal counterparts. This mechanism is known as enhanced permeation and retention (EPR).⁴¹ Moreover, with the purpose of selectively delivering the molecules into cells, functionalization of the nanoparticles' surface with bioactive molecules, such as antibodies,⁴² peptides,⁴³ folic acid,⁴⁴ aptamers,⁴⁵ allows for cell-targeting based on molecule recognition. Such systems may be designed for cytoplasmic delivery and even offer the possibility of designing robust systems for the active targeting of different cell populations.⁴⁶

1.2. Luminophores for biomedical applications

Luminescent materials are widely used for biological applications, mainly for imaging and assays, in processes where light is involved as a response in diagnostics or as the required source of photons for therapy activation (e.g. photodynamic therapy or photothermal therapy). The optical properties of biological tissues are a relevant factor to consider when developing luminescent systems for biological applications. The main chromophores present in the tissues (hemoglobin and melanin) present high absorption bands at wavelengths shorter than 600 nm and water begins to absorb significantly at wavelengths greater than 1200 nm. For these reasons, the so-called “biological transparency window” defines the range of wavelengths where the effective tissue penetration of light is maximized because of the reduced absorbance by chromophores present in the tissue. It covers the red and near-infrared (NIR) wavelengths (600–1200 nm).⁴⁷

The excitation light used to perform biomedical imaging is absorbed by the fluorescent contrast agent as well as the absorbing components present in the tissue. The latter is responsible for inducing the autofluorescence effect depending on the wavelength of irradiation. Tissue autofluorescence is a limitation when performing imaging *in vivo* as it reduces the signal to background ratio. Blue light excitation

increases tissue autofluorescence when compared to green excitation, but such an effect remains significant across the visible range. To overcome this limitation, the use of NIR light reduces fluorescence background.⁴⁸

The main conventional luminophores are organic dyes,⁴⁹ e.g. fluorescein, which is widely used in visualization of the blood flow in the vessels of the retina, choroid and iris,⁵⁰ and quantum dots (QDs),⁵¹ semiconductor nanocrystals with high intensity of luminescence, such as CdSe, CdS, and CdTe, typically 1 to 10 nm in size. These luminophores require an excitation source in the UV-visible region and emit photons of lower energy (longer wavelength), in processes involving a single photon. This is known as Stokes emission and the energy loss is called Stokes' shift. Most luminescent materials follow the Stokes' law. The inconvenient features related to this single photon process are due to the wavelength of the excitation source, which presents low penetration by the tissues and causes autofluorescence of biological tissues. Moreover, the high energy of the excitation source required may cause considerable photodamage to biological materials, such as DNA damage and cell death.⁵²

The use of luminophores that may be excited with a wavelength within the biological transparency window, as it happens with lanthanide-based upconversion nanoparticles, is a promising solution.

1.3. Lanthanide-based upconversion nanoparticles

Lanthanide-based upconversion nanoparticles (UCNPs) are currently touted as being ideal candidates for bio-probes for biological labeling and imaging because of the possibility to excite their luminescence under near infrared (NIR) illumination.⁵³ Materials based on trivalent lanthanide ions (Ln^{3+}) may present upconversion properties, e.g. visible emission obtained by excitation at NIR region in a multiphoton process. The NIR excitation matches the biological transparency window, allowing deeper tissue penetration depth due to the minimal absorption and scattering of tissues at this spectral region. Additionally, NIR excitation enables sensitive detection without the usual interference from autofluorescence background.⁵⁴ Another advantage is the lower photo-damage potential because of the low-energy of NIR photons used for excitation.⁵⁵

Multiphoton luminescence may be obtained with conventional luminophores, organic dyes^{56,57} and QDs⁵⁸. However, it requires a very high photon density, provided by a costly high-power pulsed laser, to induce the simultaneous absorption of two photons to accumulate the energy for photon upconversion. On the other hand, the Ln^{3+} -based upconversion emission results from the sequential absorption of photons due to intermediate electronic states able to store one low-energy photon until a second one arrives, thereby being possible to use low power densities to excite the upconversion emission.^{59,60}

Nanosized upconversion materials are composed of an inorganic host matrix and doping ions. The main factor in host selection is the low phonon energy to minimize non-radiative losses. The phonon energies of oxides and phosphates are quite high ($\sim 500\text{-}1000\text{ cm}^{-1}$).⁶¹ Fluorides hosts, such NaYF_4 and

NaGdF₄ present low phonon energies ($\sim 350 \text{ cm}^{-1}$) rendering them ideal hosts.⁶² UCNPs are typically doped with ytterbium (Yb³⁺) sensitizer ions, which absorb infrared radiation and non-radiatively transfer their excitation to activator ions such as erbium (Er³⁺), thulium (Tm³⁺) or holmium (Ho³⁺).⁶³ Multiplexed biological labeling can be achieved conveniently under a single wavelength excitation by changing activator ions and relative concentrations. Capabilities for the simultaneous imaging and tracking of multiple molecular targets are therefore extended, allowing the classification and differentiation of complex human diseases.⁶⁴

As UCNPs are one of the most important luminescent nanomaterials, the development of multifunctional nanosystems based on lanthanides brings a great impact in nanomedicine advances.⁶⁵ The biological application of UCNPs requires water dispersibility, biocompatibility and the possibility of subsequent surface (bio)functionalization. The post-synthetic procedures applied to hydrophobic UCNPs involve two strategies: (i) the deposition of either an additional amphiphilic or silica coating while maintaining the original hydrophobic capping on the UCNPs; (ii) the complete exchange of the original oleic acid ligands by a hydrophilic ligand.⁶⁶ Silica coating is the most common technique for nanoparticle surface modification due to its high biocompatibility. Additionally, silica is known to be highly stable and optically transparent, to present abundant Si–OH active bonds available for surface functionalization, and to have high pore volumes where drugs molecules may be stored.⁶⁷

1.4. Lanthanide-based luminescent nanothermometry

The temperature dependence of lanthanide luminescence stimulates its use for thermometry at the nanoscale. Temperature is a fundamental variable that governs diverse intracellular chemical and physical interactions in the life cycle of biological cells.⁶⁸ Measuring cell temperature allows optimization of therapeutic processes (*e.g.* hyperthermal tumor treatment).⁶⁹ Luminescence nanothermometry is a non-contact and high-resolution technique based on several kinds of materials including rare earth-doped nanoparticles, QDs and organic dyes that allow to determine intracellular temperatures within 0.5 °C.⁷⁰

A thermometer at the nanoscale may be obtained from the fluorescence signal of lanthanide ions, which is a strongly temperature-dependent effect.^{71–73} The most used dopant ion in lanthanide-based nanothermometers is Er³⁺ due to the strong temperature dependence of relative intensity of its two green luminescence bands, associated with the effect of thermal equilibrium in the population of excited states.^{74,75} The earliest work to propose the temperature sensing by using the ratio between the intensity of two emission lines, determined by a Boltzmannian population of the excited states, was made by Berthou and Jörgensen in 1990,⁷⁶ in which the upconversion-based luminescent thermometer consisted of a fluoride glass matrix co-doped with Yb³⁺ and Er³⁺ ions. The same ratiometric method was used by Maciel *et al.* in 1995 to study a new class of fluorosilicate glasses doped with Er³⁺ using a 1.48 μm continuous wave diode for excitation of visible emission.⁷⁷ As an extension to this work, the study on temperature

sensing capability of Er³⁺-doped fluoroindate glasses was further investigated for a broader temperature range from -250 to 175 °C.⁷⁸ The use of nanocrystals for temperature sensing based on the ratiometric method was reported by Alencar *et al.* in 2004.⁷⁹ The Er³⁺-doped BaTiO₃ nanocrystals were used for temperature detection by measuring the green upconverted emissions using a 980 nm diode laser as excitation source. The authors then reported that variations in surrounding medium (water, glycerol and air) and temperature (from 27.1 up to 47.1 °C) does not change the sensor sensitivity, considering the possibility of using the BaTiO₃:Er³⁺ nanocrystals in biological environments.⁸⁰ Besides working in biological fluids, thermometers for bioapplications must present resolution of the order of 0.2 °C, since temperature variations of 1 °C are very significative in biological dynamics. Additionally, the sensor should be nontoxic and soluble in water. Vetrone *et al.*⁸¹ in 2010 were able to an accurate measure of temperature in HeLa cancer cells from 25 °C to its thermally induced death at 45 °C using NaYF₄:Yb³⁺:Er³⁺ UCNPs.

Neodymium ions (Nd³⁺) are gaining attention in optical thermometry because of its transitions in NIR originated from energy levels that are thermally coupled and thus their populations follow the Boltzmann distribution. Nd³⁺ ions allow absorption and emission in the NIR spectra region, thus being more suitable for biological applications. Recently, new biological transparency windows have been identified in the over 1000 nm spectral region, aiming at bioprobes that offer deeper penetration depth to excitation light as well as deeper propagation of emitted light through biological tissues compared to existing luminophores. Despite the spectral ranges differ depending on the authors, the division considers the water absorption as well as the attenuation coefficient of human skin, blood and fatty tissue. Three distinctive regions are commonly established: the first biological window (NIR-I) from 700 nm to 950 nm, the second biological window (NIR-II) from 1000 to 1350 nm, and the third biological window (NIR-III) from 1550 to 1870 nm.⁸²⁻⁸⁵

Silva *et al.*⁸⁶ studied the photoluminescence behavior of Al₄B₂O₉:Yb³⁺:Nd³⁺ nanocrystals as a function of temperature. The samples were excited with a laser operating at 977.7 nm to obtain the upconversion emissions from 770 to 940 nm in the temperature range of 26–60 °C. In this system, Yb³⁺ participate as sensitizer in an upconversion process that involves participation of phonons, known as phonon-assisted energy transfer (PAET). In addition, Nd³⁺ may be employed as the sensitizer of upconversion luminescence under 800 nm irradiation in core-shell nanostructures owing to a cascade energy transfer process from Nd³⁺ to Yb³⁺ and a subsequent from Yb³⁺ to activator ion (Er³⁺ or Tm³⁺).⁸⁷⁻⁸⁹ This upconversion approach minimize the heating of tissues due to significant lower water absorption at 800 nm compared to conventional excitation at 980 nm. Moura *et al.*⁹⁰ reported the temperature dependence of intensity ratio between two spectral lines at 1063.5 nm and 1065.1 nm due to Nd³⁺ transitions in NdAl₃(BO₃)₄ nanocrystals by exciting at 811 nm.

The work reported by Kamimura *et al.*⁹¹ applies the ratiometric method to the emission intensity bands from two activator ions present in NaYF₄:Yb³⁺:Ho³⁺:Er³⁺ nanoparticles. The intensity ratio of the emission peaks in NIR-II (at 1150 nm of Ho³⁺) and NIR-III (at 1550 nm of Er³⁺) under NIR-I excitation (at 980 nm) showed almost linearly temperature-dependence for nanoparticles dispersed in both non-polar

and polar media (*i.e.*, cyclohexane and water, respectively) within the biological range of temperatures. The fluorescence *in vivo* imaging of a live mouse was demonstrated by injecting the PEGylated nanoparticles dispersed in physiological saline into the tail vein.

1.5. Photothermal therapy

Target cells can be suppressed through heat produced locally by a nanometric system in a therapy modality known as hyperthermia. Heating a cell above its normal temperature leads to cytotoxic effects, for instance, protein denaturation occurs at temperature greater than 39 °C and cells viability is further limited because of the aggregation of these molecules. The effects are more severe as temperature and duration of the treatment increase. For example, above 48 °C, rapid necrotic cell death takes place, bringing higher efficacy, but a lack of selectivity. For this reason, there is a clinical temperature range for hyperthermia process between 41–48 °C.⁹²

The heat induction must be well localized to ensure the selectivity of hyperthermia procedures. Localized thermal ablation of cells can be achieved by using a nanoscale material as a heater agent. Such a nanoparticle is a photoabsorber capable of efficiently generate heat under illumination with laser radiation. When light interacts with a nanoparticle, part of the incident photons are scattered and part are absorbed. The absorbed energy is released by a non-radiative pathway (heat release) or by the emission of photons of different energy (luminescence).⁹² Therefore, large absorption efficiencies and low luminescence quantum yields are some of the required features of a viable nanoheater agent.

Photothermal therapy (PTT) is an attractive therapeutic modality due to spatial specificity and minimal invasiveness, when compared to most conventional antitumor treatment techniques such as surgery, radiotherapy and chemotherapy.⁹³ UCNPs are not efficient photoabsorbers because of the low extinction coefficient of lanthanide ions, and thus are not good candidates for PTT.⁹⁴ Metallic nanoparticles can be efficient sources for local heating when illuminated at their surface plasmon resonance (SPR) band due to the enhancement of light absorption. This behaviour allows the application of these materials to convert light directly into heat and to induce localized thermal damage of a diseased tissue.^{95–97}

1.6. Multifunctional systems for luminescent thermometry and plasmonic heating

The combination of UCNPs and metal nanostructures leads to additional functionalities for potential application in PTT.^{98,99} The imaging capability of multifunctional nanosystems based on UCNPs has been used for guiding the therapy for real-time monitoring of therapeutic responses.¹⁰⁰ A temperature detector in PTT is important for better controlling the NIR irradiation to regulate the heat released to the

surrounding medium, thereby permitting guiding the therapy.¹⁰⁰⁻¹⁰¹ Recently, the combination of luminescent thermometry and plasmonic heating in single platforms for the real-time monitoring of the heat fluxes has been successfully demonstrated.⁷¹⁻¹⁰² The most recent reports published in the literature tend to shift the plasmon resonance to NIR wavelengths to match the excitation of UC by using more complex gold nanorods.¹⁰³⁻¹⁰⁵ The NIR excitation allows the use of a single laser for UC luminescence and photothermal excitation and improve the heating to reach deeper layers of tumor tissue. In addition, Debasu *et al.*¹⁰⁵ demonstrated that the use of gold nanorods instead of spherical nanoparticles allows the use of much lower (by an order of magnitude) laser power excitation densities to achieve the same temperature increase.

Taking into account the state of the art presented in literature, the main goal of this thesis was to design multifunctional platforms based on upconversion nanoparticles for applications in nanomedicine in thermometry and Au nanoparticles-based photothermal therapy.

References

-
- 1 PRASAD, P. N. **Introduction to nanomedicine and nanobioengineering**. New Jersey: John Wiley & Sons, 2012.
 - 2 RIEHEMANN, K.; SCHNEIDER, S. W.; LUGER, T. A.; GODIN, B.; FERRARI, M.; FUCHS, H. Nanomedicine—challenge and perspectives. **Angew. Chem. Int. Ed.**, v. 48, p. 872–897, 2009.
 - 3 ZHANG, X.-Q.; XU, X.; BERTRAND, N.; PRIDGEN, E.; SWAMI, A.; FAROKHZAD, O. C. Interactions of nanomaterials and biological systems: Implications to personalized nanomedicine. **Adv. Drug. Deliv. Rev.**, v. 64, p. 1363–1384, 2012.
 - 4 SHIN, T.-H.; CHEON, J. Synergism of nanomaterials with physical stimuli for biology and medicine. **Acc. Chem. Res.**, v. 50, p. 567–572, 2017.
 - 5 SHI, J.; KANTOFF, P. W.; WOOSTER, R.; FAROKHZAD, O. C. Cancer nanomedicine: Progress, challenges and opportunities. **Nat. Rev. Cancer**, v. 17, p. 20–37, 2017.
 - 6 CHAN, W. C. W. Nanomedicine 2.0. **Acc. Chem. Res.**, v. 50, p. 627–632, 2017.
 - 7 NEL, A. E.; MÄDLER, L.; VELEGOL, D.; XIA, T.; HOEK, E. M.; SOMASUNDARAN, P.; KLAESSIG, F.; CASTRANOVA, V.; THOMPSON, M. Understanding biophysicochemical interactions at the nano-bio interface. **Nat. Mat.**, v. 8, p. 543–557, 2009.
 - 8 CHOI, H. S.; LIU, W.; MISRA, P.; TANAKA, E.; ZIMMER, J. P.; IPE, B. I.; BAWENDI, M. G.; FRANGIONI, J. V. Renal clearance of nanoparticles. **Nat Biotechnol.**, v. 25, p. 1165–1170, 2007.
 - 9 LONGMIRE, M.; CHOYKE, P. L.; KOBAYASHI, H. Clearance properties of nano-sized particles and molecules as imaging agents: Considerations and caveats. **Nanomedicine**, v. 3, p. 703–717, 2008.

-
- 10 ALLEN, T. M.; CULLIS, P. R. Drug delivery systems: entering the mainstream. **Science**, v. 303, p. 1818–1822, 2004.
- 11 DENG, Y.; CAI, Y.; SUN, Z.; LIU, J.; LIU, C.; WEI, J.; LI, W.; LIU, C.; WANG, Y.; ZHAO, D. Multifunctional mesoporous composite microspheres with well-designed nanostructure: a highly integrated catalyst system. **J. Am. Chem. Soc.**, v. 132, p. 8466–8473, 2010.
- 12 LI, C.; ZHANG, Y.; CHEN, G.; HU, F.; ZHAO, K.; WANG, Q. Engineered multifunctional nanomedicine for simultaneous stereotactic chemotherapy and inhibited osteolysis in an orthotopic model of bone metastasis. **Adv. Mater.**, v. 29, p. 1605754–1605754, 2017.
- 13 MOHAMMADI, M.; RAMEZANI, M.; ABNOUS, K.; ALIBOLANDI, M. Biocompatible polymersomes-based cancer theranostics: Towards multifunctional nanomedicine. **Int. J. Pharm.**, v. 519, p. 287–303, 2017.
- 14 GAO, J.; GU, H.; XU, B. Multifunctional magnetic nanoparticles: Design, synthesis, and biomedical applications. **Acc. Chem. Res.**, v. 42, p. 1097–1107, 2009.
- 15 GYAWALI, D.; PALMER, M.; TRAN, R. T.; YANG, J. Progress of nanobiomaterials for theranostic systems. In: TIWARI, A.; RAMALINGAM, M.; HISATOSHI K.; TURNER, A. P. F. **Biomedical materials and diagnostic devices**. Beverly: Scrivener Publishing LLC, 2012. chap. 14, p. 435–476.
- 16 CINTEZA, L. O. Multifunctional nanosystems for cancer theragnostics. **Biomedical Optics and Medical Imaging. SPIE Newsroom**, v. 10, p. 003432, 2011.
- 17 ZHOU, F.; HUANG, L. Liposome-mediated cytoplasmic delivery of proteins: An effective means of accessing the MHC class I-restricted antigen presentation pathway. **Immunomethods**, v. 4, p. 229–235, 1994.
- 18 BALASUBRAMANIAN, V. ONACA, O.; ENEA, R.; HUGHES, D. W.; PALIVAN, C. G. Protein delivery: From conventional drug delivery carriers to polymeric nanoreactors. **Expert Opin. Drug Deliv.**, v. 7, p. 63–78, 2010.
- 19 WANG, Z.; LIU, G.; ZHENG, H.; CHEN, X. Rigid nanoparticle-based delivery of anti-cancer siRNA: Challenges and opportunities. **Biotechnol. Adv.**, v. 32, p. 831–843, 2014.
- 20 FADEEL, B.; GARCÍA-BENNETT, A.E. Better safe than sorry: Understanding the toxicological properties of inorganic nanoparticles manufactured for biomedical applications. **Adv. Drug Deliver. Rev.**, v. 62, p. 362–374, 2010.
- 21 HUANG, X.; LI, L.; LIU, T.; HAO, N.; LIU, H.; CHEN, D.; TANG, F. The shape effect of mesoporous silica nanoparticles on biodistribution, clearance, and biocompatibility in vivo. **ACS Nano**, v. 5, p. 5390–5399, 2011.
- 22 LLOPIS-LORENTE, A.; LOZANO-TORRES, B.; BERNARDOS, A.; MARTÍNEZ-MÁÑEZ, R.; SANCENÓN, F. Mesoporous silica materials for controlled delivery based on enzymes. **J. Mater. Chem. B**, v. 5, p. 3069–3083, 2017.
- 23 DE OLIVEIRA, L. F.; BOUCHMELLA, K.; GONÇALVES, K. D. A.; BETTINI, J.; KOBARG, J.; CARDOSO, M. B. Functionalized silica nanoparticles as an alternative platform for targeted drug-delivery of water insoluble drugs. **Langmuir**, v. 32, 3217–3225, 2016.
- 24 VIVERO-ESCOTO, J. L.; SLOWING, I. I.; TREWYN, B. G.; LIN, V. S. Y. Mesoporous silica nanoparticles for intracellular controlled drug delivery. **Small**, v. 6, p. 1952–1967, 2010.

-
- 25 WU, S. H.; MOU, C. Y.; LIN, H. P. Synthesis of mesoporous silica nanoparticles. **Chem. Soc. Rev.**, v. 42, p. 3862–3875, 2013.
- 26 DE OLIVEIRA FREITAS, L. B. BRAVO, I. J. G.; DE ALMEIDA MACEDO, W. A.; DE SOUSA, E. M. B. Mesoporous silica materials functionalized with folic acid: Preparation, characterization and release profile study with methotrexate. **J. Sol-Gel Sci. Technol.**, v. 77, p. 186–204, 2016.
- 27 ZHANG, Z.; ZHANG, X.; NIU, D.; LI, Y.; SHI, J. Large-pore, silica particles with antibody-like, biorecognition sites for efficient protein separation. **J. Mater. Chem. B**, v. 5, p. 4214–4220, 2017.
- 28 ZOU, Z.; HE, D.; CAI, L.; HE, X.; WANG, K.; YANG, X.; LI, L.; LI, S.; SU, X. Alizarin complexone functionalized mesoporous silica nanoparticles: A smart system integrating glucose-responsive double-drugs release and real-time monitoring capabilities. **ACS Appl. Mater. Interfaces**, v. 8, p. 8358–8366, 2016.
- 29 SHEN, D.; YANG, J.; LI, X.; ZHOU, L.; ZHANG, R.; LI, W.; CHEN, L.; WANG, R.; ZHANG, F.; ZHAO, D. Biphase stratification approach to three-dimensional dendritic biodegradable mesoporous silica nanospheres. **Nano Lett.**, v. 14, p. 923–932, 2014.
- 30 CHENG, W.; NIE, J.; XU, L.; LIANG, C.; PENG, Y.; LIU, G.; WANG, T.; MEI, L.; HUANG, L.; ZENG, X. A pH-sensitive delivery vehicle based on folic acid-conjugated polydopaminemodified mesoporous silica nanoparticles for targeted cancer therapy. **ACS Appl. Mater. Interfaces**, v. 9, p. 18462–18473, 2017.
- 31 KURCH, S.; SCHLÖDER, J.; BERGES, C.; OSE, R.; SCHUPP, J.; TUETTENBERG, A.; WEISS, H.; SCHULTZE, J.; WINZEN, S.; SCHINNERER, M.; KOYNOV, K.; MEZGER, M.; HAASS, N. K.; TREMEL, W.; JONULEIT, H. Dendritic mesoporous silica nanoparticles for pH-stimuli-responsive drug delivery of TNF-alpha. **Adv Healthc. Mater.**, v. 6, p. 1700012, 2017.
- 32 CHEN, X. YUAN, P.; LIU, Z.; BAI, Y.; ZHOU, Y. Dual responsive hydrogels based on functionalized mesoporous silica nanoparticles as an injectable platform for tumor therapy and tissue regeneration. **J. Mater. Chem. B**, v. 5, p. 5968–5973, 2017.
- 33 DONG, J.; ZINK, J. I. Light or heat? The origin of cargo release from nanoimpeller particles containing upconversion nanocrystals under IR irradiation. **Small**, v. 11, p. 4165–4172, 2015.
- 34 AZNAR, E.; MONDRAGÓN, L.; ROS-LIS, J. V.; SANCENÓN, F.; MARCOS, M. D.; MARTÍNEZ-MÁÑEZ, R.; SOTO, J.; PÉREZ-PAYÁ, E.; AMORÓS, P. Finely tuned temperature-controlled cargo release using paraffin-capped mesoporous silica nanoparticles. **Angew Chem Int Ed Engl.**, v. 50, p. 11172–11175, 2011.
- 35 MAL, N. K.; FUJIWARA, M.; TANAKA, Y. Photocontrolled reversible release of guest molecules from coumarin-modified mesoporous silica. **Nature**, v. 421, p. 350–353, 2003.
- 36 CHAI, S.; GUO, Y.; ZHANG, Z.; CHAI, Z.; MA, Y.; QI, L. Cyclodextrin-gated mesoporous silica nanoparticles as drug carriers for red light-induced drug release. **Nanotechnology**, v. 28, p. 145101, 2017.
- 37 RUIZ-HERNÁNDEZ, E.; BAEZA, A.; VALLET-REGÍ, M. Smart drug delivery through DNA/magnetic nanoparticle gates. **ACS Nano**, v. 5, p. 1259–1266, 2011.
- 38 ZHANG, J.; YUAN, Z. F.; WANG, Y.; CHEN, W. H.; LUO, G. F.; CHENG, S. X.; ZHUO, R. X.; ZHANG, X. Z. Multifunctional envelope-type mesoporous silica nanoparticles for tumor-triggered targeting drug delivery. **J. Am. Chem. Soc.**, v. 135, p. 5068–5073, 2013.

-
- 39 LEE, J.; HAN, S.; LEE, J.; CHOI, M.; KIM, C. Stimuli-responsive α -helical peptide gatekeepers for mesoporous silica nanocarriers. **New J. Chem**, v. 41, p. 6969–6972, 2017.
- 40 SONG, Y.; LI, Y.; XU, Q.; LIU, Z. Mesoporous silica nanoparticles for stimuli-responsive controlled drug delivery: Advances, challenges, and outlook. **Int. J. Nanomedicine**, v. 12, p. 87–110, 2017.
- 41 FERRARI, M. Cancer nanotechnology: Opportunities and challenges, **Nat. Rev. Cancer**, v. 5, p. 161–171, 2005.
- 42 KUMAR, S.; AARON, J.; SOKOLOV, K. Directional conjugation of antibodies to nanoparticles for synthesis of multiplexed optical contrast agents with both delivery and targeting moieties. **Nat. Protoc.**, v. 3, p. 314–320, 2008
- 43 AMIN, M.; BADIEE, A.; JAAFARI, M. R. Improvement of pharmacokinetic and antitumor activity of PEGylated liposomal doxorubicin by targeting with N-methylated cyclic RGD peptide in mice bearing C-26 colon carcinomas. **Int. J. Pharm.**, v. 458, p. 324–333, 2013.
- 44 LU, J.; ZHAO, W.; HUANG, Y.; LIU, H.; MARQUEZ, R.; GIBBS, R. B.; LI, J.; VENKATARAMANAN, R.; XU, L.; LI, S. Targeted delivery of doxorubicin by folic acid-decorated dual functional nanocarrier. **Mol. Pharm.**, v. 11, p. 4164–4178, 2014.
- 45 OH, S. S.; LEE, B. F.; LEIBFARTH, F. A.; EISENSTEIN, M.; ROBB, M. J.; LYND, N. A.; HAWKER, C. J.; SOH, H. T. Synthetic aptamer-polymer hybrid constructs for programmed drug delivery into specific target cells. **J. Am. Chem. Soc.**, v. 136, p. 15010–15015, 2014.
- 46 BALE, S. S.; KWON, S. J.; SHAH, D. A.; BANERJEE, A.; DORDICK, J. S.; KANE, R. S. Nanoparticle-mediated cytoplasmic delivery of proteins to target cellular machinery. **ACS Nano**, v. 4, p. 1493–1500, 2010.
- 47 HAMBLIN, M. R.; DEMIDOVA, T. N. Mechanisms of low level light therapy. In: HAMBLIN, M. R.; WAYNANT, R. W.; ANDERS, J. (Ed.). **Mechanisms of low level light therapy**. Bellingham: SPIE – The International Society for Optical Engineering, 2006. v. 6140, p. 614001/1-614001/12.
- 48 FRANGIONI, J. V. *In vivo* near-infrared fluorescence imaging. **Current Opinion in Chem. Biol.**, v. 7, p. 626–634, 2003.
- 49 SAMEIRO, M.; GONÇALVES, T. Fluorescent labeling of biomolecules with organic probes. **Chem. Rev.**, v. 109, p. 190–212, 2009.
- 50 BERKOW, J. W.; FLOWER, R. W.; ORTH, D. H.; KELLEY, J. S. **Fluorescein and indocyanine green angiography**: technique and interpretation. 2nd ed. San Francisco: The Foundation of the American Academy of Ophthalmology, 1997.
- 51 MEDINTZ, I. L.; UYEDA, H. T.; GOLDMAN, E. R.; MATTOUSSI, H. Quantum dot bioconjugates for imaging, labelling and sensing. **Nat. Mater.**, v. 4, p. 435–446, 2005.
- 52 ZHOU, J.; LIU, Z.; LI, F. Upconversion nanophosphors for small-animal imaging. **Chem. Soc. Rev.**, v. 41, p. 1323–1349, 2012.
- 53 LIU, Q.; FENG, W.; LI, F. Water-soluble lanthanide upconversion nanophosphors: synthesis and bioimaging applications *in vivo*. **Coord. Chem. Rev.**, v. 273-274, p. 100–110, 2014.
- 54 TU, D.; ZHENG, W.; LIU, Y.; ZHU, H.; CHEN, X. Luminescent biodetection based on lanthanide-doped inorganic nanoprobos. **Coord. Chem. Rev.**, v. 273-274, p. 13–29, 2014.

-
- 55 YUAN, P.; LEE, Y. H.; GNANASAMMANDHAN, M. K.; GUAN, Z.; ZHANG, Y.; XU, Q. H. Plasmon enhanced upconversion luminescence of NaYF₄:Yb,Er@SiO₂@Ag core-shell nanocomposites for cell imaging. **Nanoscale**, v. 4, p. 5132–5137, 2012.
- 56 WANG, X. L.; KREBS, J.; AL-NURI, M. H.; PUDAVAR, E.; GHOSAL, S.; LIEBOW, C.; NAGY, A. A.; SCHALLY, A. V.; PRASAD, P. N. A chemically labeled cytotoxic agent: two-photon fluorophore for optical tracking of cellular pathway in chemotherapy. **Proc. Natl. Acad. Sci. U. S. A.**, v. 96, p. 11081–11084, 1999.
- 57 MOREAUX, L.; SANDRE, O.; CHARPAK, S.; BLANCHARD-DESCE, M.; MERTZ, J. Coherent scattering in multi-harmonic light microscopy. **Biophys. J.**, v. 80, 1568, 2001.
- 58 PADILHA, L.A. FU, J.; HAGAN, D. J.; VAN STRYLAND, E. W.; CESAR, C. L.; BARBOSA, L. C.; CRUZ, C. H. Two-photon absorption in CdTe quantum dots. **Opt. Express**, v. 13, p. 6460–6467. 2005.
- 59 AUZEL, F. Upconversion and anti-stokes processes with f and d ions in solids. **Chem. Rev.**, v. 104, p. 139–173, 2004.
- 60 BETTINELLI, M.; CARLOS, L.; LIU, X. Lanthanide-doped upconversion nanoparticles. **Phys. Today**, v. 68, p. 38–44, 2015.
- 61 WANG, F.; LIU, X. Recent advances in the chemistry of lanthanide-doped upconversion nanocrystals. **Chem. Soc. Rev.**, v. 38, p. 976–989, 2009.
- 62 XU, C. T.; ZHAN, Q.; LIU, H.; SOMESFALEAN, G.; QIAN, J.; HE, S.; ANDERSSON-ENGELS, S. Upconverting nanoparticles for pre-clinical diffuse optical imaging, microscopy and sensing: Current trends and future challenges. **Laser and Photonics Rev.**, v. 7, p. 663–697, 2013.
- 63 ZHAO, J.; JIN, D.; SCHARTNER, E. P.; LU, Y.; LIU, Y.; ZVYAGIN, A. V.; ZHANG, L.; DAWES, J. M.; XI, P.; PIPER, J. A.; GOLDYS, E. M.; MONRO, T. M. Single-nanocrystal sensitivity achieved by enhanced upconversion luminescence. **Nat. Nanotech.**, v. 8, p. 729–734, 2013.
- 64 DOANE, T. L.; BURDA, C. The unique role of nanoparticles in nanomedicine: imaging, drug delivery and therapy. **Chem. Soc. Rev.**, v. 41, p. 2885–2911, 2012.
- 65 WANG, H.; HAN, R. L.; YANG, L. M.; SHI, J. H.; LIU, Z. J.; HU, Y.; WANG, Y.; LIU, S. J.; GAN, Y. Design and synthesis of core-shell-shell upconversion nanoparticles for NIR-induced drug release, photodynamic therapy, and cell imaging. **ACS Appl. Mater. Interfaces**, v. 8, p. 4416–4423, 2016.
- 66 WILHELM, S.; KAISER, M.; WÜRTH, C.; HEILAND, J.; CARRILLO-CARRION, C.; MUHR, V.; WOLFBEIS, O. S.; PARAK, W. J.; RESCH-GENGER, U.; HIRSCH, T. Water dispersible upconverting nanoparticles: effects of surface modification on their luminescence and colloidal stability. **Nanoscale**, v. 7, p. 1403–10, 2015.
- 67 LI, C.; HOU, Z.; DAI, Y.; YANG, D.; CHENG, Z.; MA, P.; LIN, J. A facile fabrication of upconversion luminescent and mesoporous core-shell structured β -NaYF₄:Yb³⁺, Er³⁺@mSiO₂ nanocomposite spheres for anti-cancer drug delivery and cell imaging. **Biomater. Sci.**, v. 1, p. 213–223, 2013.
- 68 ZOHAR, O.; IKEDA, M.; SHINAGAWA, H.; INOUE, H.; NAKAMURA, H.; ELBAUM, D.; ALKON, D. L.; YOSHIOKA, T. Thermal imaging of receptor-activated heat production in single cells. **Biophys. J.**, v. 74, p. 82–89, 1998.
- 69 HUANG, H.; DELIKANLI, S.; ZENG, H.; FERKEY, D. M.; PRALLE, A. Remote control of ion channels and neurons through magnetic-field heating of nanoparticles. **Nat. Nanotechnol.**, v. 5, p. 602–606, 2010.

-
- 70 GOTTA, C.; OKABE, K.; FUNATSU, T.; HARADA, Y.; UCHIYAMA, S. Hydrophilic fluorescent nanogel thermometer for intracellular thermometry. **J. Am. Chem. Soc.**, v. 131, p. 2766–2767, 2009.
- 71 DEBASU, M. L.; ANANIAS, D.; PASTORIZA-SANTOS, I.; LIZ-MARZÁN, L. M.; ROCHA, J.; CARLOS, L. D. All-in-one optical heater-thermometer nanoplatform operative from 300 to 2000 K based on Er³⁺ emission and blackbody radiation. **Adv. Mater.**, v. 25, p. 4868–4874, 2013.
- 72 BRITES, C. D. S.; LIMA, P. P.; SILVA, N. J. O.; MILLÁN, A.; AMARAL, V. S.; PALACIO, F.; CARLOS, L. D. Thermometry at the nanoscale. **Nanoscale**, v. 4, p. 4799–4829, 2012.
- 73 BRITES, C. D. S.; LIMA, P. P.; SILVA, N. J. O.; MILLÁN, A.; AMARAL, V. S.; PALACIO, F.; CARLOS, L. D. A luminescent molecular thermometer for long-term absolute temperature measurements at the nanoscale. **Adv. Mater.**, v. 22, p. 4499–4504, 2010.
- 74 WADE, S. A.; COLLINS, S. F.; BAXTER, G. W. Fluorescence intensity ratio technique for optical fiber point temperature sensing. **J. Appl. Phys.**, v. 94, p. 4743–4756, 2003.
- 75 ZHANG, F. Upconversion nanoparticles for thermal sensing. In: _____. **Photon Upconversion Nanomaterials**. Berlin: Springer-Verlag, 2015. chap. 10, p. 343–374.
- 76 BERTHOUS, H.; JÖRGENSEN, C. K. Optical-fiber temperature sensor based on upconversion-excited fluorescence. **Opt. Lett.**, v. 15, p. 1100–1102, 1990.
- 77 MACIEL, G. S.; MENEZES, L. de S.; GOMES, A. S. L.; de ARAÚJO, C. B.; MESSADDEQ, Y.; FLOREZ, A.; AEGERTER, M. A. Temperature sensor based on frequency upconversion in Er³⁺-doped fluoroindate glass. **IEEE Photon. Technol. Lett.**, v. 7, p. 1474–1476, 1995.
- 78 MACIEL, G. S.; de ARAÚJO, C. B.; MESSADDEQ, Y.; AEGERTER, M. A. Frequency upconversion in Er³⁺-doped fluoroindate glasses pumped at 1.48 μm. **Phys. Rev. B**, v. 55, p. 6335–6342, 1997.
- 79 ALENCAR, M. A. R. C.; MACIEL, G. S.; de ARAÚJO, C. B.; PATRA, A. Er³⁺-doped BaTiO₃ nanocrystals for thermometry: Influence of nanoenvironment on the sensitivity of a fluorescence based temperature sensor. **Appl. Phys. Lett.**, v. 84, p. 4753–4755, 2004.
- 80 MACIEL, G. S.; ALENCAR, M. A. R. C.; de ARAÚJO, C. B.; PATRA, A. Upconversion emission of BaTiO₃:Er³⁺ nanocrystals: influence of temperature and surrounding medium. **J. Nanosci. Nanotechnol.**, v. 10, p. 2143–2148, 2010.
- 81 VETRONE, F.; NACCACHE, R.; ZAMARRON, A.; SANZ-RODRIGUEZ, F.; MAESTRO, L. M.; RODRIGUEZ, E. M.; JAQUE, D.; SOLE, J. G.; CAPOBIANCO, J. A. Temperature sensing using fluorescent nanothermometers. **ACS Nano**, v. 4, p. 3254–3258, 2010.
- 82 HEMMER, E.; BENAYAS, A.; LÉGARÉ, F.; VETRONE, F. Exploiting the biological windows: current perspectives on fluorescent bioprobes emitting above 1000 nm. **Nanoscale Horiz.**, v. 1, p. 168–184, 2016.
- 83 SMITH, A. M.; MANCINI, M. C.; NIE, S. Second window for *in vivo* imaging. **Nat Nanotechnol.**, v. 4, p. 710–711, 2009.
- 84 JAQUE, D.; RICHARD, C.; VIANA, B.; SOGA, K.; LIU, X.; GARCÍA SOLÉ, J. Inorganic nanoparticles for optical bioimaging. **Adv. Opt. Photonics**, v. 8, p. 1–103, 2016.

-
- 85 DIAO, S.; BLACKBURN, J. L.; HONG, G.; ANTARIS, A. L.; CHANG, J.; WU, J. Z.; ZHANG, B.; CHENG, K.; KUO, C. J.; DAI, H. Fluorescence imaging in vivo at wavelengths beyond 1500 nm. **Angew. Chem. Int. Ed.**, v. 54, p. 14758–14762, 2015.
- 86 SILVA, A. F.; ELAN, F.; FALCÃO-FILHO, E. L.; MAIA, L. J. Q.; de ARAÚJO, C. B. Thermal sensitivity of frequency upconversion in $\text{Al}_4\text{B}_2\text{O}_9:\text{Yb}^{3+}/\text{Nd}^{3+}$ nanoparticles. **J. Mater. Chem. C**, v. 5, p. 1240–1246, 2017.
- 87 XIMENDES, E. C.; ROCHA, U.; JACINTO, C.; KUMAR, K. U.; BRAVO, D.; LOPEZ, F. J.; RODRIGUEZ, E. M.; GARCIA-SOLE, J.; JAQUE, D. Self-monitored photothermal nanoparticles based on core–shell engineering. **Nanoscale**, v. 8, p. 3057–3066, 2016.
- 88 JIANG, G.; ZHOU, S.; WEI, X.; CHEN, Y.; DUAN, C.; YIN, M.; YANG, B.; CAO, W. 794 nm excited core–shell upconversion nanoparticles for optical temperature sensing. **RSC Adv.**, v. 6, p. 11795–11801, 2016.
- 89 CHEN, W.; SHI, C.; TAO, T.; JI, M.; ZHENG, S.; SANG, X.; LIU, X.; QIU, J. Optical temperature sensing with minimized heating effect using core–shell upconversion nanoparticles. **RSC Adv.**, v. 6, p. 21540–21545, 2016.
- 90 MOURA, A. L.; PINCHEIRA, P. I. R.; MAIA, L. J. Q.; GOMES, A. S. L.; de ARAÚJO, C. B. Two-color random laser based on a Nd^{3+} doped crystalline powder. **J. Lumin.**, v. 181, p. 44–48, 2017.
- 91 KAMIMURA, M.; MATSUMOTO, T.; SUYARI, S.; UMEZAWA, M.; SOGA, K. Ratiometric near-infrared fluorescence nanothermometry in the OTN-NIR (NIR II/III) biological window based on rare-earth doped $\beta\text{-NaYF}_4$ nanoparticles. **J. Mater. Chem. B**, v. 5, p. 1917–1925, 2017.
- 92 JAQUE, D.; MARTÍNEZ MAESTRO, L.; ROSAL, B. DEL; HARO-GONZALEZ, P.; BENAYAS, A.; PLAZA, J. L.; MARTÍN RODRÍGUEZ, E.; GARCÍA SOLÉ, J. Nanoparticles for photothermal therapies. **Nanoscale**, v. 6, p. 9494–9530, 2014.
- 93 EL-SAYED, I. H.; HUANG, X.; EL-SAYED, M. A. Selective laser photo-thermal therapy of epithelial carcinoma using anti-EGFR antibody conjugated gold nanoparticles. **Cancer Letters**, v. 239, p. 129–135, 2006.
- 94 CHEN, G.; QIU, H.; PRASAD, P. N.; CHEN, X. Upconversion nanoparticles: Design, nanochemistry, and applications in Theranostics. **Chem. Rev.**, v. 114, p. 5161–5214, 2014.
- 95 HUANG, X.; JAIN, P. K.; EL-SAYED, I. H.; EL-SAYED, M. A. Plasmonic photothermal therapy (PPTT) using gold nanoparticles. **Laser Med. Sci.**, v. 23, p. 217–228, 2008.
- 96 CHERUKURI, P.; GLAZER, E. S.; CURLEY, S. A. Targeted hyperthermia using metal nanoparticles. **Adv. Drug Delivery Rev.**, v. 62, p. 339–345, 2010.
- 97 LAL, S.; CLARE, S. E.; HALAS, N. J. Nanoshell-enabled photothermal cancer therapy: impending clinical impact. **Acc. Chem. Res.**, v. 41, p. 1842, 2008.
- 98 CHENG, L.; YANG, K.; LI, Y.; CHEN, J.; WANG, C.; SHAO, M.; LEE, S.-T.; LIU, Z. Facile preparation of multifunctional upconversion nanoprobe for multimodal imaging and dual-targeted photothermal therapy. **Angew. Chem. Int. Ed.**, v. 50, p. 7385–7390, 2011.
- 99 CHENG, L.; YANG, K.; LI, Y.; ZENG, X.; SHAO, M.; LEE, S.-T.; LIU, Z. Multifunctional nanoparticles for upconversion luminescence/MR multimodal imaging and magnetically targeted photothermal therapy. **Biomaterials**, v. 33, p. 2215–2222, 2012.

-
- 100 DONG, B.; XU, S.; SUN, J.; BI, S.; LI, D.; BAI, X.; WANG, Y.; WANG, L.; SONG, H. Multifunctional NaYF₄:Yb³⁺,Er³⁺@Ag core/shell nanocomposites: integration of upconversion imaging and photothermal therapy. **J. Mater. Chem.**, v. 21, p. 6193–6200, 2011.
- 101 MAESTRO, L. M.; HARO, P.; IGLESIAS-DE LA CRUZ, M. C.; SANZ-RODRÍGUEZ, F.; JUARRANZ, Á.; SOLÉ, J. G.; JAQUE, D. Fluorescent nanothermometers provide controlled plasmonic-mediated intracellular hyperthermia. **Nanomedicine**, v. 8, p. 379–388, 2013.
- 102 BRITES, C. D. S.; FUERTES, M. C.; ANGELOMÉ, P. C.; MARTÍNEZ, E. D.; LIMA, P. P.; SOLER-ILLIA, G. J.; CARLOS, L. D. Tethering luminescent thermometry and plasmonics: Light manipulation to assess real-time thermal flow in nanoarchitectures. **Nano Lett.**, v. 17, p. 4746–4752, 2017.
- 103 HUANG, Y.; ROSEI, F.; VETRONE, F. A single multifunctional nanoplatform based on upconversion luminescence and gold nanorods. **Nanoscale**, v. 7, p. 5178–5185, 2015.
- 104 ROHANI, S.; QUINTANILLA, M.; TUCCIO, S.; DE ANGELIS, F.; CANTELAR, E.; GOVOROV, A. O.; RAZZARI, L.; VETRONE, F. Enhanced luminescence, collective heating, and nanothermometry in an ensemble system composed of lanthanide-doped upconverting nanoparticles and gold nanorods. **Adv. Opt. Mater.**, v. 3, p. 1606–1613, 2015.
- 105 DEBASU, M. L.; BRITES, C. D.; BALABHADRA, S.; OLIVEIRA, H.; ROCHA, J.; CARLOS, L. D. Nanoplatforms for plasmon-induced heating and thermometry. **ChemNanoMat**, v. 2, p. 520–527, 2016.

Chapter 8.

Conclusions

In summary, two main multifunctional systems were developed in this thesis work. The first one combined an optical heater and a temperature probe. The design was based on AuNSs with the surface decorated with UCNPs. AuNSs were used to produce heat when illuminated at their SPR band in the NIR aiming for the use of the produced heat to induce well-localized thermal damage of cancer cells in PTT. In this work we were able to measure the temperature increase induced by the AuNSs by monitoring the Yb³⁺-Er³⁺ upconversion emission, showing the potential of the system for guiding PTT process, in which a temperature detector with high spatial resolution is necessary, to minimize the damage of surrounding tissues.

The second system developed is a dual-mode nanothermometer combined with an UV light sensor. These multifunctional nanoparticles displayed temperature-dependent emissions in the visible region from both UV pumped downshifting Eu³⁺ luminescence and NIR pumped Yb³⁺-Er³⁺ upconversion. In addition, the Eu³⁺ emission intensity presented an exponential decay with exposure time and is therefore sensitive to the UV exposure dose, indicating its potential to guide UV light activated therapies.

Since both systems are essentially based on UCNPs of NaGdF₄ doped with the ions Yb³⁺-Er³⁺, the first part of the work was mainly focused on the synthesis conditions *via* thermal decomposition of fluoride precursors. The structure and morphology were investigated to establish the synthetic protocol to obtain monodisperse nanocrystals in the pure hexagonal phase, which is known to present higher emission intensity. The luminescence properties of cubic and hexagonal crystal phases were compared. The UCNPs in the hexagonal phase showed to be more suitable for application as a temperature sensor than the cubic phase, due to its lower red-to-green emission ratio and higher thermal sensitivity.

After studying the structural and optical properties of the hydrophobic oleate-capped nanocrystals, the phase transfer to aqueous media was necessary with regards to their intended use for biological applications. The surface of UCNPs was modified by coating with a thin silica shell. The method based on reverse microemulsion route was optimized to prevent silica interparticle polymerisation might otherwise affect water dispersability. Dynamic light scattering analysis of micellar systems at different stages of synthesis and of the final nanoparticles was performed. Optimized reaction parameters comprised: UCNPs initial concentration; surfactant and TEOS concentration, reaction time, centrifugation speed and catalyst (dimethyl ammonium or ammonium hydroxide). A uniform silica shell on the nanocrystal surface was obtained. The core-shell UCNPs presented the property of converting infrared

energy into visible light and offered suitable properties for application as a temperature sensor. Optical characterization in the vicinity of the physiological range revealing excellent temperature sensing linearity.

The next step was the coupling of UCNPs core-silica shell onto the surface of metal core-silica shell nanoparticles. Three strategies were investigated for the fabrication of UCNP-metal nanocomposites: (i) through a covalent “click” cycloaddition methodology;¹ (ii) based on electrostatic interaction between anionic UCNPs@SiO₂ and the positively charged metallic surface obtained by modification with the polyelectrolyte poly(diallyldimethylammonium chloride) (PDADMAC);² (iii) by functionalization of UCNPs@SiO₂ with amine groups. The latter coupling strategy showed the best results. However, the most important factor was the comparative size of the nanocomponents. Initially, silica coated silver nanoparticles with a silver core diameter of 70 nm were used to develop the synthesis protocol, but these studies were further extended to gold and silver nanostructures with different shapes (spheres, rods and shells). Ultimately, UCNPs@SiO₂ of about 40 nm could be successfully coupled with much larger gold nanoshells of around 300 nm.

The heating properties of the obtained AuNSs@UCNPs nanocomposites were demonstrated by irradiating the colloidal solution at different laser power to excite the SPR of Au and by measuring the Yb³⁺-Er³⁺ upconversion emission spectra. In the presence of AuNSs the temperature reached around 40 °C. The multifunctional system behaved as a combined heater and a temperature sensor under NIR excitation.

The functionalities of the UCNPs@SiO₂ nanothermometers were then extended by adding a second active luminescent center. The attachment of a Eu³⁺/tta complex to the silica shell was confirmed by the observation of the characteristic and unique luminescence properties (photoluminescence excitation and emission spectra), which agreed with data published in the literature for the well-known complex [Eu(tta)₃(H₂O)₂], and a composite that was prepared from an organic-inorganic hybrid host and the complex (presented in Figure 6.2). It must be said that the small amount of complex was not detectable by infrared vibrational spectroscopy or Raman spectroscopy. The Eu³⁺ emission spectrum of the obtained UCNPs@SiO₂-Eu(tta)₃ showed a broadening of emission lines compared to literature spectra. Such broadening in Eu³⁺ complexes when grafted to different surfaces is well known and is mostly due to the contribution of coordinating groups from the surface (silanol groups for example) to the Eu³⁺ first coordination sphere in the case of the complex considered here by substituting for water molecules in the Eu³⁺ coordination sphere. To support this hypothesis, results obtained by us before for a completely different host (organic-inorganic “ureasil” hybrid) are instructional. In that case, the contribution from oxygen atoms to the host is considered. The identification of the grafted species as “Eu(tta)₃” could be considered oversimplifying, but we do think that it introduces important errors or misconceptions. The exact formulation for the grafted species should be established in a systematic spectroscopic study for each host studied.

Temperature determination using the Eu³⁺ system presents a drawback compared to Er³⁺, since a nonratiometric thermal parameter is used. Ratiometric methods are indeed more reliable and present

many advantages in comparison with those based on the intensity of only one transition due to their self-referencing feature. However, the Eu^{3+} -based thermal sensor proposed in this work presented suitable features, such as the linear luminescence thermal dependence and quite high thermal sensitivity.

However, we did not observe UV degradation of the Eu^{3+} -based thermometer, since a linear correlation was observed, whereas the correlation is known to be exponential in the case of UV degradation. The effects of UV degradation on luminescence intensity decay are different for each sensor due to different mechanisms. For UV sensing, degradation of the tta ligand hinders the antenna effect and is thus responsible for the intensity exponential decay. Meanwhile, for temperature sensing, the Eu^{3+} energy levels are directly influenced by effects such as: redistribution of electronic state population, quenching mechanisms and non-radiative transitions. It must be pointed out that the incident UV power was 5x larger for the degradation tests compared with the temperature measurements.

Optimization of UV light activated therapeutic processes is necessary to minimize the detrimental effects associated with overexposure, such as DNA damage. We proposed a UV light sensor to ensure that the effective dose is delivered to the patient by controlling the exposure time for a given UV power density. As UV light intensity and experimental setup were constant over the measurement time, it is possible to determine the time required to reduce the Eu^{3+} emission intensity to 50% (from the curve presented in Figure 6.7). This result may be extrapolated for different power density values.

This thesis brings original and interesting results concerning the use of lanthanides for sensing applications based on lanthanide luminescence, and stimulates the study of multifunctional materials. The new materials presented in this work could find interesting applications in luminescent thermometry under ultraviolet or near-infrared excitation, UV light sensing, as well as photodynamic therapy and photothermal therapy. The new nanoplateforms are dispersible in aqueous environment, thus being attractive for applications in nanomedicine for guiding light activated therapies to avoid photodamage and overheating of normal tissues.

References

1 ASSELIN, J.; ROY, C.; BOUDREAU, D.; MESSADDEQ, Y.; BOUCHAREB, R.; MATHIEU, P. Supported core-shell nanobiosensors for quantitative fluorescence imaging of extracellular pH. **Chem. Commun.**, v. 50, p. 13746–13749, 2014.

2 MA, Z.; DING, T. Bioconjugates of glucose oxidase and gold nanorods based on electrostatic interaction with enhanced thermostability. **Nanoscale Res. Lett.**, v. 4, p. 1236–1240, 2009.